Cancer Immunology Research

Virotherapy with a Semliki Forest Virus–Based Vector Encoding IL12 Synergizes with PD-1/PD-L1 Blockade

José I. Quetglas, Sara Labiano, M. Ángela Aznar, Elixabet Bolaños, Arantza Azpilikueta, Inmaculada Rodriguez, Erkuden Casales, Alfonso R. Sánchez-Paulete, Víctor Segura, Cristian Smerdou, and Ignacio Melero

Abstract

Virotherapy and checkpoint inhibitors can be combined for the treatment of cancer with complementarity and potential for synergistic effects. We have developed a cytolytic but nonreplicative viral vector system based on Semliki Forest virus that encodes IL12 (SFV-IL12). Following direct intratumoral injection, infected cells release transgenic IL12, die, and elicit an inflammatory response triggered by both abundantly copied viral RNA and IL12. In difficult-to-treat mouse cancer models, such as those derived from MC38 and bilateral B16-OVA, SFV-IL12 synergized with an anti–PD-1 monoclonal antibody (mAb) to induce tumor regression and prolong survival. Similar synergistic effects were attained upon PD-L1 blockade. Combined SFV-IL12 + anti–PD-1 mAb treatment only marginally increased the elicited cytotoxic T-lymphocyte response over SFV-IL12 as a single agent, at least when measured by *in vivo* killing assays. In contrast, we observed that SFV-IL12 treatment induced expression of PD-L1 on tumor cells in an IFNγ-dependent fashion. PD-L1–mediated adaptive resistance thereby provides a mechanistic explanation of the observed synergistic effects achieved by the SFV-IL12 + anti–PD-1 mAb combination. *Cancer Immunol Res; 3(5); 449–54. ©2015 AACR.*

Introduction

Semliki Forest virus (SFV)–based RNA viral vectors have been developed for vaccination and immunotherapy of cancer (1, 2). These propagation-deficient vectors can accommodate expression cassettes and have been engineered to encode cytokines and other proimmunogenic transgenes. A SFV vector encoding the heterodimeric murine interleukin-12 (IL12; SFV-IL12) proteins (3–5) under the control of two independent subgenomic promoters is a powerful antitumor agent when directly injected into experimental tumors (6). The effect is the result of killing tumor cells in an immunogenic fashion, the local effects of the IL12 transgene, and the innate immune activation caused by viral RNA, including a powerful type I IFN response (7). In a previous study, we observed that SFV-IL12 and agonist costimulatory antibodies injected intratumorally (i.t.) and directed against the lymphocyte surface receptor CD137 were markedly synergistic (8).

Cancer immunotherapy is currently being revolutionized by the advent of monoclonal antibodies (mAb) blocking PD-1 and its PD-L1 ligand (9–11). Such antibodies exert antitumor effects in numerous mouse models and have shown frequent durable objective responses in melanoma, renal cell carcinoma, non–small cell lung cancer, and other malignancies (12–14).

In this study, we explored the combination of the local proimmunogenic effects of SFV-IL12 along with the relief of the coinhibitory restraints mediated by PD-1 on the antitumor cytotoxic T-lymphocyte (CTL) response. Potent synergistic effects of the combination were observed with evidence for PD-L1 induction on tumor cells by the IL12–IFNγ axis. Such a train of events results in escape mechanisms that are tackled by anti–PD-1 mAb upon combination.

Materials and Methods

Cell lines and animals

The BHK-21 cell line (ATCC CCL-10) was cultured as described previously (4). The murine melanoma cell line B16.F10 and the OVA-expressing variant B16-OVA (H-2^b), the MC38 mouse adenocarcinoma cell line and the 4T1 murine breast cancer cell line, were tested to be *Mycoplasma* free and verified for identity. Five-week-old female C57BL/6 and Balb/c mice were purchased from Harlan Laboratories. Animal studies were approved by the institutional ethics committee for animal experimentation under Spanish regulations (protocol number 071-13).

Vector production

Plasmids pSFV-enhLacZ and pSFV-enhIL12 have been described previously (4, 15). Plasmid pSFV-NS3 encodes the cytoplasmic Hepatitis C virus NS3 protein (C. Smerdou and

Division of Immunology and Immunotherapy, Center for Applied Medical Research (CIMA), and University Clinic, University of Navarra, Pamplona, Navarra, Spain.

Note: Supplementary data for this article are available at Cancer Immunology Research Online (http://cancerimmunolres.aacrjournals.org/).

Corresponding Authors: Ignacio Melero, Division of Immunology and Immunotherapy, Center for Applied Medical Research (CIMA), and University Clinic, University of Navarra, Av Pio XII, 55, Pamplona, Navarra 31008, Spain. Phone: 00-34-9481-94700; Fax: 00-34-9481-94717; E-mail: imelero@unav.es; and Jose I. Quetglas, jquetglas@unav.es

doi: 10.1158/2326-6066.CIR-14-0216

colleagues; unpublished results). RNA synthesis from SFV plasmids, transfection into BHK-21 cells by electroporation, and packaging of recombinant RNA into SFV viral particles (vp) were performed as described previously (16, 17). Briefly, BHK-21 cells were coelectroporated with recombinant RNA and two helper RNAs (i.e., SFV-helper-C-S219A and SFV-helper-S2 RNAs), which provided *in trans* the SFV capsid and spike proteins, respectively (17). SFV vp were harvested and purified by ultracentrifugation as described previously (18). Indirect immunofluorescence was applied to SFV-infected BHK-21 cells to determine the titer of SFV-NS3, SFV-enhLacZ, and SFV-enhIL12 (the last two designated in this article as SFV-LacZ and SFV-IL12, respectively) recombinant virus stocks as described previously (19). Viral vectors were kept frozen at −80°C until use.

Induction and treatment of tumor nodules

Mice were s.c. injected with B16-OVA, B16.F10, MC38, and 4T1 cells (5×10^5 cells per animal) in the right flank. Mice injected with B16-OVA or B16.F10 cells were injected again in the contralateral flank 6 days following the first inoculation in the right flank. Treatments were administered 6 to 10 days following tumor cell inoculation as detailed for each experiment. SFV-LacZ and SFV-IL12 were resuspended in 25 μL of PBS and injected i.t. with 28-G needles. Three doses of 100 μg of anti–PD-1 mAb (clone RMP1-14; Bio X Cell) and/or anti-CD137 mAb (clone 1D8, kindly provided by Maria Jure-Kunkel, BMS) or anti–PD-L1 mAb (10B5, hybridoma) were administered i.p. as detailed for each experiment. The efficacy of treatment was evaluated by measuring the size of tumor nodules every 3 to 4 days.

***In vivo* killing assay**

Splenocytes from naïve C57BL/6 mice were stained with 5 μmol/L of Violet Proliferation Dye 450 (BD Biosciences) and then divided into three different samples. Two of these samples were pulsed with 10 μg/mL of the $OVA_{257–264}$ peptide (SIINFEKL, NeoMPS) or the TRP-$2_{180–188}$ peptide (SVYDFFVWL, NeoMPS) for 30 minutes at 37°C in 5% CO_2 and extensively washed. The third sample received no peptide as an additional control. OVA-pulsed, TRP-2–pulsed, and nonpulsed splenocytes were then labeled with 1 μmol/L ($CFSE^{hi}$), 100 nmol/L ($CFSE^{med}$), or 10 nmol/L ($CFSE^{low}$) of CFSE (Sigma-Aldrich) and with Violet Proliferation Dye 450 (BD Horizon) at 10 μmol/L in all cases. The three samples were mixed at the same ratio and injected i.v. (3×10^6 cells of each population) into B16-OVA–bearing or naïve mice. Twenty hours later, spleens were harvested, and the transferred target cells were identified and gated using Violet Proliferation Dye 450. Specific cytotoxicity was analyzed by flow cytometry and calculated as follows: 100 − [100 × (% $CFSE^{hi}$ or $CFSE^{med}$ tumor–bearing mice/% $CFSE^{low}$ tumor–bearing mice)/(%$CFSE^{hi}$ or $CFSE^{med}$ naïve mice/% $CFSE^{low}$ naïve mice)].

***In vivo* induction of PD-L1 expression on tumor cells**

B16-OVA tumors were generated as described above and inoculated with 10^8 vp of SFV-LacZ, or SFV-IL12, or an equivalent volume of saline. SFV-IL12–injected mice also received 1 mg of a blocking anti-IFNγ mAb (clone HB170, hybridoma) or an equivalent volume of saline i.p. After 3 days, tumors were harvested and treated with 400 U/mL collagenase D and 50 μg/mL DNase I (Roche Diagnostics). After mechanical tissue dissociation, cells were passed through a 70-μm nylon mesh filter (BD Falcon, BD Bioscience) and washed. Cells were also treated with ACK lysing buffer and washed before further use. Finally, cell suspensions were immunostained to assess H2-K^b and PD-L1 expression on gated CD45-negative malignant cells by flow cytometry.

***In vitro* induction of PD-L1 expression on tumor cells**

B16-OVA cells were plated in triplicate in 12-well cell culture plates at a seeding density of 5×10^4 cells per well. When cells had attached to the wells, 3 hours later, fresh splenocytes from C57BL/6 mice were added or not at three different B16-OVA/splenocytes ratios: 1:1, 1:5, and 1:10. Supernatants from SFV-enhIL12– or SFV-NS3–infected BHK cells were added to the cell cocultures, in the presence or absence of a blocking anti-IFNγ mAb (clone HB170, hybridoma) at 10 μg/mL. As an additional negative control, B16-OVA cells without splenocytes were similarly treated and analyzed. As a positive control, B16-OVA cells were cultured in the presence of 10^3 U/mL of IFNγ (Miltenyi Biotec). Three days later, B16-OVA cells were collected, washed with PBS, and analyzed for H2-K^b and PD-L1 surface expression on gated CD45-negative populations.

Flow cytometry

Single-cell suspensions obtained from *in vivo* growing tumors or *in vitro* experiments were pretreated with anti-CD16/32 mAbs (clone 2.4G2; BD Biosciences Pharmingen) to reduce nonspecific binding to Fc receptors. Then, cells were stained as needed with the following fluorochrome-conjugated antibodies: CD45.2 (100), PD-L1 (10F.9G2), and H2-K^b (AF6-88.5) purchased from Biolegend. Dead cells were discarded during the analysis by staining with Sytox Green or 7-AAD (Molecular Probes). A FACS-Canto II (BD-Biosciences) was used for cell acquisition, and data analysis was carried out using FlowJo software (TreeStar Inc.).

Statistical analyses

All error terms are expressed as SD. Prism software (GraphPad Software Inc.) was used for statistical analysis. Survival of tumor-bearing animals was represented by Kaplan–Meier curves and analyzed by log-rank tests. Data were analyzed first by the Kolmogorov–Smirnov normality test. The Kruskal–Wallis tests followed by Dunn multiple comparison tests were used to permit comparisons in experiments with four experimental groups. *P* values of <0.05 were considered to be statistically significant. The synergy index (S) was studied using the formula described by Mazat and colleagues (20).

Results

SFV-IL12 and anti–PD-1 mAb synergistic effects

To test the combined effects of i.t. SFV-IL12 and anti–PD-1 mAb blockade, we chose the B16-OVA bilateral melanoma model. In this setting, mice were s.c. inoculated twice with tumor cells in each flank with a 6-day interval between injections. On day 10, SFV-LacZ or SFV-IL12 was given i.t. in the nodule firstly induced, along with systemic anti–PD-1 mAb or saline given on days 10, 13, and 17. Figure 1A shows the progression of individual tumors and demonstrates that combined treatment was superior to achieve control of the bilateral experimental disease, resulting in an evident survival advantage

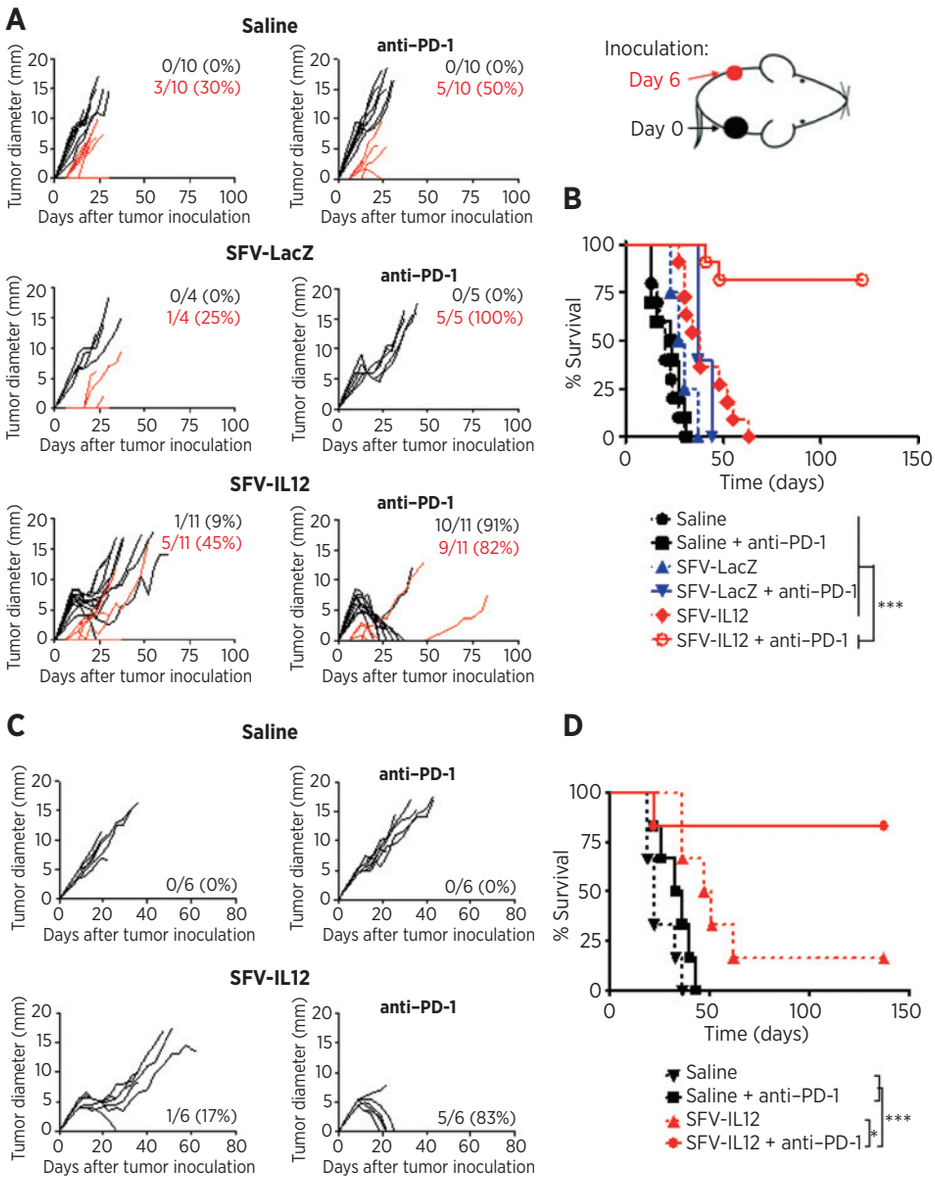

Figure 1.
Treatment efficacy of SFV-IL12 + anti–PD-1 combination. A, C57BL/6 female mice were inoculated s.c. with 5×10^5 B16-OVA cells in the right flank on day 0 and in the left flank on day 6, as indicated in the drawing. They then received an intratumoral injection of saline (top), 10^8 vp of SFV-LacZ (middle), or 10^8 vp of SFV-IL12 (bottom) on day 10 as indicated. On days 10, 13, and 17, mice received i.p. 100 μg of anti–PD-1 mAb (right), or an equivalent volume of vehicle (left). Black curves signify follow-up of the directly SFV-IL12–treated tumor diameters (tumors in the right flank); red curves, follow-up of the nontreated tumor diameter (left tumors). Each curve represents an individual mouse. The fractions in black in the right upper corner of each graph indicate the number of rejected treated tumors, and fractions in red indicate the number of rejected contralateral tumors relative to the total number of animals in each group, with the percentage of complete tumor regressions. C, C57BL/6 female mice were inoculated s.c. in the right flank with 5×10^5 MC38 cells on day 0 and then received an intratumoral injection of saline (top), or 10^8 vp of SFV-IL12 (bottom) on day 9. On days 9, 12, and 16, mice received i.p. 100 μg of anti–PD-1 mAb (right), or an equivalent volume of saline vehicle (left). Each curve represents the evolution of the mean tumor diameter for each individual mouse. The numbers in the right lower corner of each graph indicate the fraction of tumor-free mice on day 80 relative to the total number of animals in each group, and the percentage of complete tumor regressions, respectively. B and D, Kaplan–Meier plots of mouse survival. The SFV-IL12 + anti–PD-1–treated group was compared with the rest of the groups with the log-rank test. *, $P < 0.05$; ***, $P < 0.001$. In panels A and B, the graphs correspond to pooled data of two independent experiments with similar results.

(Fig. 1B) with over 80% of mice remaining completely tumor free at the end of the experiment. According to the formula of the synergy index (S) described by Mazat and colleagues (20), we calculated an S value of +9.11, clearly superior to zero. Therefore, we can conclude that SFV-IL12 + anti–PD-1 synergized to reject treated tumors completely.

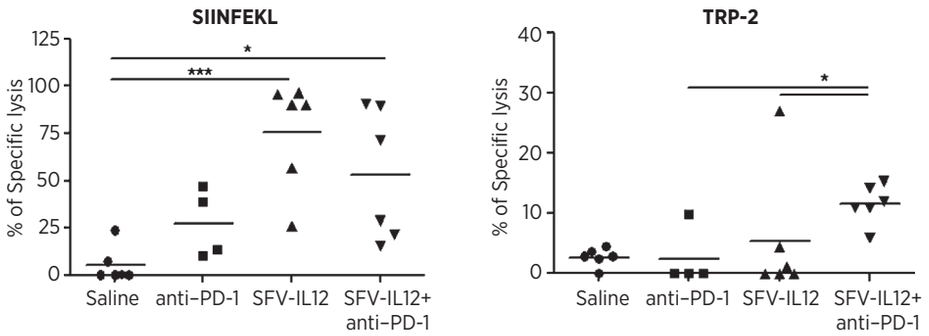

Figure 2.

Minor enhancements in *in vivo* killing assays induced by SFV-IL12 + antiPD-1 mAb combined treatment. C57BL/6 female mice were s.c. inoculated with 5×10^5 B16-OVA cells on day 0 and then received i.t. saline or 10^8 vp of SFV-IL12 on day 10. On days 10 and 13, mice received i.p. 100 μg of anti–PD-1 mAb or an equivalent volume of saline. On day 17, tumor-antigen peptide-pulsed splenocytes from naïve mice were injected as target cells into treated mice. Twenty hours later, mice were sacrificed and spleens were collected. The percentage of specific cell lysis was quantified by flow cytometry. Specific *in vivo* cytotoxicity against SIINFEKL-pulsed targets (left) and against SVYDFFVWL (TRP-2)–pulsed targets is indicated for each individual mouse with the mean of the group represented by a horizontal line. *, $P < 0.05$; ***, $P < 0.001$.

Such synergistic effects were also observed upon treatment of MC38-derived tumors that were injected with a suboptimal dose of SFV-IL12 that by itself only cured 1 of 6 mice (Fig. 1C). However, upon treatment with the combined regimen, most of the mice were completely cured in an experimental setting in which anti–PD-1 mAb as a single agent only resulted in a marginal retardation of tumor growth with no survival benefit (Fig. 1D). In this experiment, a positive S (+3.88) value was computed, thus demonstrating a synergistic rather than a merely additive effect of the combined treatment. Again, a majority of mice treated with the combination were tumor free at the end of the experiment.

The PD-1/PD-L1 pathway is targeted in the clinic with agents directed against either one of these counter receptors. In our combination regimen, we tested in parallel both options (anti–PD-1 or anti–PD-L1 mAb) and obtained similar results on B16-OVA–derived tumors (Supplementary Fig. S1).

These experiments were extended to the untransfected bilateral B16.F10 tumor model and the 4T1 breast cancer model. In both instances, a less evident but reproducible therapeutic effect was observed with the combined treatment (Supplementary Fig. S2A and S2B). In the case of 4T1-derived breast carcinomas, a group of mice was treated with a triple combination of SFV-IL12 i.t. + anti–PD-1 + anti-CD137 mAbs with a trend suggestive of better survival (Supplementary Fig. S2B). Our data strongly support synergistic therapeutic effects of i.t. injection of SFV-IL12 with PD-1 blockade that were exerted both against the SFV-IL12–injected tumor and distantly implanted lesions that were not injected with the viral vector.

Immune mechanisms driving the SFV-IL12 + anti–PD-1 synergy

Both SFV-IL12 and anti–PD-1 mAbs rely on amplified CTL antitumor responses to exert therapeutic effects (4, 21). Hence, an alternative explanation for the combined effects could be the induction or amplification of a more robust antitumor CTL response. In the same therapeutic setting of Fig. 1A and B, we performed *in vivo* killing experiments testing CTLs against the OVA-derived peptide SIINFEKL and an endogenous melanosomal peptide antigen (TRP-2) also presented by H2-K^b. The results indicated only a marginal improvement in cytotoxicity with the combination regimen on the CTL response in the case of the TRP-2 antigen but none in the case of the OVA-derived antigen (Fig. 2). In the case of the OVA epitope, SFV-IL12 as a single agent induced a nearly optimal response, which is difficult to be improved upon by the PD-1 blockade. Of note, PD-1 as a single agent induced a very modest increase in CTL responses, at least in this difficult-to-treat tumor model. Thus, we reasoned that the cooperative mechanism for synergy ought to be different and hypothesized that the virally encoded IL12 could act as an inducer of PD-L1 on tumor cells via IFNγ (21), thereby resulting in a tumor-protective factor against CTLs as elicited by SFV-IL12.

Indeed, as shown in Fig. 3A and B, SFV-IL12 i.t. injection induced bright expression of PD-L1 on CD45-negative tumor cells analyzed by flow cytometry. This was paralleled by a concomitant increase in the surface expression of MHC class I molecules. Induction of both MHC-I and PD-L1 only took place with the vector encoding IL12 but not with a similar SFV vector encoding β-galactosidase as a control transgene. Moreover, IFNγ blockade *in vivo* with a neutralizing mAb abolished the induction of both PD-L1 and MHC-I. Similar results were observed in MC38-derived tumors (data not shown). Therefore, IL12 induction of IFNγ in the tissue microenvironment is responsible for the induction of PD-L1 and MHC-I. Although PD-L1 would be detrimental for CTL tumor destruction (22), MHC I would probably enhance tumor-antigen presentation.

This train of phenomena could be mimicked in cell cultures, for example, the coculturing B16-OVA melanoma cells with syngeneic splenocytes as a putative source of IFNγ in response to IL12. Indeed, when such cocultures were supplemented with virus-free and IL12-containing supernatants from BHK cells that had been infected with SFV-IL12, tumor cells increased their surface expression of MHC I (data not shown) and PD-L1, an effect that was also abolished with the addition of an anti-IFNγ mAb to neutralize this cytokine as produced by the cocultured lymphocytes (Fig. 3C and D).

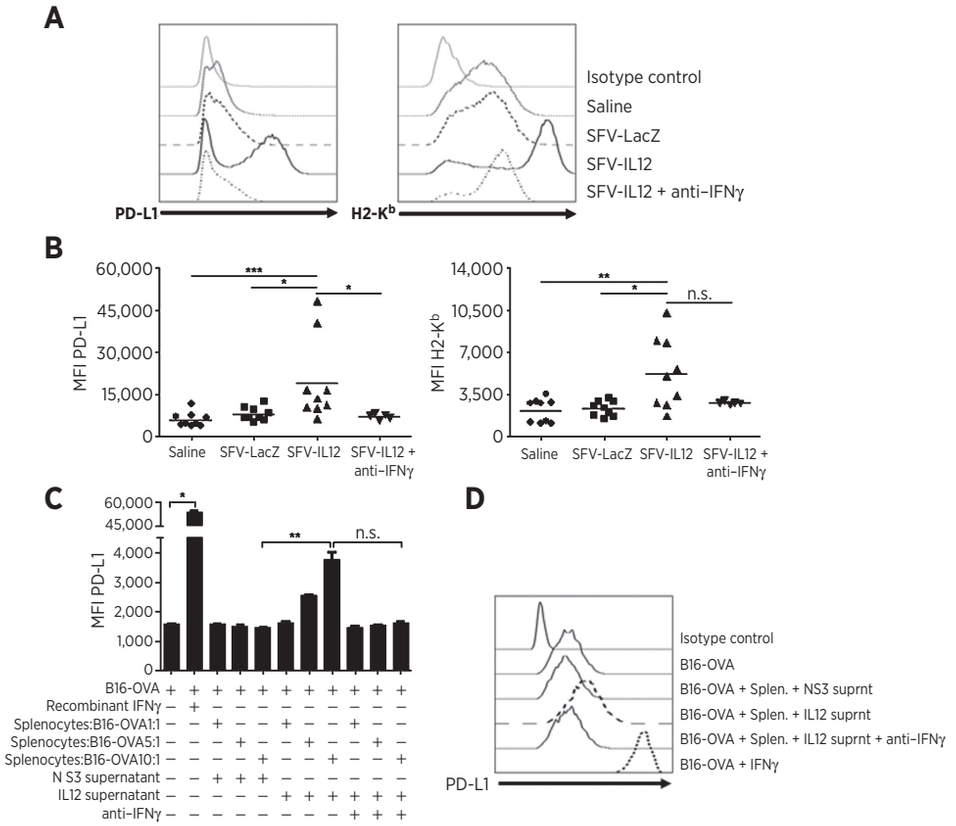

Figure 3.
Induction of PD-L1 expression on tumor cells is mediated by IFNγ. A and B, study of PD-L1 and H2-K^b expression on B16-OVA tumor cells. C57BL/6 mice were s.c. inoculated with 5×10^5 B16-OVA cells on day 0. On day 10, mice were injected i.t. with saline, or 10^8 vp of SFV-LacZ, or 10^8 vp of SFV-IL12. In addition, a group of SFV-IL12–inoculated mice received i.p. 1 mg of anti-IFNγ mAb or an equivalent volume of vehicle. At 72 hours after vector inoculation, mice were sacrificed and tumors were excised for the evaluation of H2-K^b and PD-L1 surface expression by flow cytometry. A, histograms showing the expression of PD-L1 (left) and H2-K^b (right) on CD45.2-negative tumor cells of one representative mouse per group. B, graphs showing mean fluorescence intensity (MFI) of PD-L1 (left) or H2-K^b (right) immunostainings gated on CD45.2-negative tumor cells for each individual mouse with the mean of the group represented by a horizontal line. The graphs represent pooled data from two independent experiments with similar results. C and D, study of PD-L1 expression on B16-OVA cells *in vitro*. B16-OVA cells were cultured alone or cocultured in triplicate with different ratios of splenocytes from a naïve C57BL/6 mouse. Supernatants of control SFV-NS3– or SFV-IL12–infected cells were added to the cocultures. Recombinant IFNγ (10^3 U/mL) as a positive control or anti-IFNγ mAb (10 μg/mL) were added when indicated. C, graph showing the MFI of PD-L1–positive cells gated on CD45.2-negative cells. D, histograms showing the expression of PD-L1 on CD45.2-negative cells as observed in one representative well per condition. *, $P < 0.05$; **, $P < 0.01$; ***, $P < 0.001$; Isot. ctrl., isotype control; n.s., not statistically significant; Splen., splenocytes; Suprnt., supernatant.

Discussion

This study provides strong preclinical evidence to combine virotherapy and checkpoint blockade for cancer treatment. Previous results have pointed to the synergistic effects of tumoral infection with Newcastle disease virus and blockade with anti–CTLA-4 mAbs (23). Immunostimulatory mAbs directed against CD137 to enforce T-cell costimulation are also strongly synergistic with intratumoral Vaccinia virus–derived vectors (24) and SFV-IL12 (8).

Viral vectors, even if not replicative, mimic an acute pathogenic viral infection, sending a compendium of alarm signals that call for a CTL-mediated immune response (25). We hypothesize that mimicking viral infection of the tumor should trigger or sustain the proper type of cytotoxic inflammation in the tumor microenvironment. With this rationale in mind, checkpoint inhibitors operating in the malignant tissue can unleash the efficacy of CTL response that had resulted from tumor infection or from the expression of proimmunogenic transgenes, such as IL12.

In this study, an undesirable loop is elicited by SFV-IL12, which, in an IFNγ-mediated fashion, induces PD-L1 on tumor cells. Hypoxia via HIF1α may also contribute to PD-L1 overexpression (21) because IL12 is known for its antiangiogenic effects (3). We have observed that blockade of such adaptive resistance mechanisms results in powerful synergistic effects that can control distant tumor lesions not treated with the viral SFV vector.

Combinations of local virotherapy and systemic checkpoint blockade are suitable for testing first in metastatic melanoma with accessible cutaneous metastasis, in which treatment is provided to one or some of the lesions in an attempt to turn transduced lesions into an *in situ* cancer vaccine (26). Combined strategies of this kind, based on knowledge of the

immunodynamic interaction of the viral vector and checkpoint blocking antibody, hold much promise for clinical translation because both types of agents are currently undergoing clinical trials.

Disclosure of Potential Conflicts of Interest

I. Melero reports receiving a commercial research grant from Pfizer and is a consultant/advisory board member for Bristol-Myers Squibb, Roche-Genentech, and AstraZeneca. No potential conflicts of interest were disclosed by the other authors.

Authors' Contributions

Conception and design: J.I. Quetglas, I. Melero
Development of methodology: J.I. Quetglas, C. Smerdou, I. Melero
Acquisition of data (provided animals, acquired and managed patients, provided facilities, etc.): J.I. Quetglas, M.Á. Aznar, E. Bolaños, A. Azpilikueta, E. Casales
Analysis and interpretation of data (e.g., statistical analysis, biostatistics, computational analysis): J.I. Quetglas, V. Segura, I. Melero
Writing, review, and/or revision of the manuscript: J.I. Quetglas, S. Labiano, M.Á. Aznar, A.R. Sánchez-Paulete, V. Segura, C. Smerdou, I. Melero
Administrative, technical, or material support (i.e., reporting or organizing data, constructing databases): J.I. Quetglas, S. Labiano, M.Á. Aznar, E. Bolaños, A. Azpilikueta, I. Rodriguez, E. Casales, A.R. Sánchez-Paulete
Study supervision: J.I. Quetglas, I. Melero

Acknowledgments

The authors thank Drs. J.L. Perez-Gracia, J. Prieto, S. Hervas-Stubbs, J.J. Lasarte, and S. Martín-Algarra for scientific discussion and long-term collaborations in the development of combined immunotherapies. The authors also thank Dr. Diego Alignani for flow cytometry support and Eneko Elizalde for excellent animal facility care.

Grant Support

This study was financially supported by MICINN (SAF2008-03294 and SAF2011-22831, to I. Melero) and FIS (PI11/02190 and PI14/01442, to C. Smerdou). I. Melero was also funded by the Departamento de Salud del Gobierno de Navarra, Redes temáticas de investigación cooperativa RETICC, and European Commission VII Framework Program (ENCITE and IACT).

Received November 17, 2014; revised January 29, 2015; accepted February 9, 2015; published OnlineFirst February 17, 2015.

References

1. Quetglas JI, Ruiz-Guillen M, Aranda A, Casales E, Bezunartea J, Smerdou C. Alphavirus vectors for cancer therapy. Virus Res 2010;153:179–96.
2. Smerdou C, Liljestrom P. Non-viral amplification systems for gene transfer: vectors based on alphaviruses. Curr Opin Mol Ther 1999;1:244–51.
3. Sangro B, Melero I, Qian C, Prieto J. Gene therapy of cancer based on interleukin 12. Curr Gene Ther 2005;5:573–81.
4. Rodriguez-Madoz JR, Prieto J, Smerdou C. Semliki forest virus vectors engineered to express higher IL-12 levels induce efficient elimination of murine colon adenocarcinomas. Mol Ther 2005;12:153–63.
5. Rodriguez-Madoz JR, Liu KH, Quetglas JI, Ruiz-Guillen M, Otano I, Crettaz J, et al. Semliki forest virus expressing interleukin-12 induces antiviral and antitumoral responses in woodchucks with chronic viral hepatitis and hepatocellular carcinoma. J Virol 2009;83:12266–78.
6. Quetglas JI, Rodriguez-Madoz JR, Bezunartea J, Ruiz-Guillen M, Casales E, Medina-Echeverz J, et al. Eradication of liver-implanted tumors by Semliki Forest virus expressing IL-12 requires efficient long-term immune responses. J Immunol 2013;190:2994–3004.
7. Melero I, Quetglas JI, Reboredo M, Dubrot J, Rodriguez-Madoz JR, Mancheño U, et al. Strict requirement for vector-induced type I interferon in efficacious antitumor responses to virally encoded IL12. Cancer Res 2015;75:497–507.
8. Quetglas JI, Dubrot J, Bezunartea J, Sanmamed MF, Hervas-Stubbs S, Smerdou C, et al. Immunotherapeutic synergy between anti-CD137 mAb and intratumoral administration of a cytopathic Semliki Forest virus encoding IL-12. Mol Ther 2012;20:1664–75.
9. Topalian SL, Drake CG, Pardoll DM. Targeting the PD-1/B7-H1(PD-L1) pathway to activate anti-tumor immunity. Curr Opin Immunol 2012;24: 207–12.
10. Perez-Gracia JL, Labiano S, Rodriguez-Ruiz ME, Sanmamed MF, Melero I. Orchestrating immune check-point blockade for cancer immunotherapy in combinations. Curr Opin Immunol 2014;27:89–97.
11. Sznol M, Chen L. Antagonist antibodies to PD-1 and B7-H1 (PD-L1) in the treatment of advanced human cancer—response. Clin Cancer Res 2013; 19:5542.
12. Topalian SL, Hodi FS, Brahmer JR, Gettinger SN, Smith DC, McDermott DF, et al. Safety, activity, and immune correlates of anti-PD-1 antibody in cancer. N Engl J Med 2012;366:2443–54.
13. Brahmer JR, Tykodi SS, Chow LQ, Hwu WJ, Topalian SL, Hwu P, et al. Safety and activity of anti-PD-L1 antibody in patients with advanced cancer. N Engl J Med 2012;366:2455–65.
14. Robert C, Ribas A, Wolchok JD, Hodi FS, Hamid O, Kefford R, et al. Anti-programmed-death-receptor-1 treatment with pembrolizumab in ipilimumab-refractory advanced melanoma: a randomised dose-comparison cohort of a phase 1 trial. Lancet 2014;384:1109–17.
15. Quetglas JI, Fioravanti J, Ardaiz N, Medina-Echeverz J, Baraibar I, Prieto J, et al. A Semliki forest virus vector engineered to express IFNalpha induces efficient elimination of established tumors. Gene Ther 2012; 19:271–8.
16. Liljestrom P, Garoff H. A new generation of animal cell expression vectors based on the Semliki Forest virus replicon. Biotechnology 1991;9:1356–61.
17. Smerdou C, Liljestrom P. Two-helper RNA system for production of recombinant Semliki forest virus particles. J Virol 1999;73:1092–8.
18. Fleeton MN, Sheahan BJ, Gould EA, Atkins GJ, Liljestrom P. Recombinant Semliki Forest virus particles encoding the prME or NS1 proteins of louping ill virus protect mice from lethal challenge. J Gen Virol 1999;80:1189–98.
19. Salminen A, Wahlberg JM, Lobigs M, Liljestrom P, Garoff H. Membrane fusion process of Semliki Forest virus. II: cleavage-dependent reorganization of the spike protein complex controls virus entry. J Cell Biol 1992; 116:349–57.
20. Mazat F, Langla J, Mazat JP. The measure of synergy in enzymatic regulation. A general coefficient. Biochimie 1981;63:107–11.
21. Noman MZ, Desantis G, Janji B, Hasmim M, Karray S, Dessen P, et al. PD-L1 is a novel direct target of HIF-1alpha, and its blockade under hypoxia enhanced MDSC-mediated T cell activation. J Exp Med 2014;211:781–90.
22. Azuma T, Yao S, Zhu G, Flies AS, Flies SJ, Chen L. B7-H1 is a ubiquitous antiapoptotic receptor on cancer cells. Blood 2008;111:3635–43.
23. Zamarin D, Holmgaard RB, Subudhi SK, Park JS, Mansour M, Palese P, et al. Localized oncolytic virotherapy overcomes systemic tumor resistance to immune checkpoint blockade immunotherapy. Sci Transl Med 2014;6: 226ra32.
24. John LB, Howland LJ, Flynn JK, West AC, Devaud C, Duong CP, et al. Oncolytic virus and anti-4-1BB combination therapy elicits strong antitumor immunity against established cancer. Cancer Res 2012;72:1651–60.
25. Pandey S, Kawai T, Akira S. Microbial sensing by toll-like receptors and intracellular nucleic acid sensors. Cold Spring Harb Perspect Biol 2014;7: pii: a016246.
26. Marabelle A, Kohrt H, Caux C, Levy R. Intratumoral immunization: a new paradigm for cancer therapy. Clin Cancer Res 2014;20:1747–56.